Deflected-Lamina Electrophoresis (DLE): High Performance Separation of Biologicals in Space

Allen Strickler*
Beckman Instruments, Inc., Anaheim, Calif.

In the familiar planar form of continuous electrophoresis, an electric field is applied edge-to-edge across a flowing sheet of buffer into which a sample is injected as a continuous filamentary stream. A less familiar alternative is to apply a field normal to the buffer plane and to introduce the sample as a broad, thin "lamina." The sample is split into separate "leaves" as the fractions migrate at different angles toward one of the walls. An advantage here is the capacity for high processing rates. Reported performance to date has been limited, however, by the narrow deflection space, cell design difficulties, and an incomplete understanding of phenomena affecting cell behavior. Several developments now permit a more promising assessment of this "deflected lamina" approach: an analysis that has clarified underlying phenomena, improved construction techniques, and, most important, the availability of microgravity. Using buffer layers 4-6 mm or more thick, it appears feasible in microgravity to combine useful resolution with processing rates 25- to 100-fold higher than conventionally possible in 1 *g*. An alternative capability is that of using buffer media of high conductivity, approximating that of physiological media, although at lowered throughput. A rocket flight experiment has been proposed that will verify flow stability in moderately thick, electrically heated buffer layers, and fractionate biological cells by the deflected lamina technique.

Introduction

ELECTROPHORESIS in free liquid media is acknowledged to be of high potential value in the separation of biological cells and cellular components. Its capabilities in Earth gravity are limited, however, by convective disturbance and the tendency of sample particles to settle. Microgravity provides an escape from these limitations, opening the prospect of a high-performance capability serving important needs in medicine and biological research.

A favored approach to electrophoresis in space has been the use of a continuous planar method.[1-3] A fine flowing filament of sample is introduced into a thin flowing layer of electrolyte, then separated into a steady-state fan of components by applying a dc field across the width of the layer. Typical performance for this approach in 1 *g* is illustrated by Fig. 1 (solid line). Resolution is defined here as the reciprocal of the least resolvable mobility difference, the latter expressed in the units shown. The vertical dotted lines represent the range of desirable resolution as stated by Seaman.[4] The system is capable of moderate sample throughput rates, i.e., about 20 μ litres/min at the lower levels of useful resolution, assuming a buffer ionic strength of about 0.01. With such buffers, the system accepts up to several percent concentration of solids in the sample. At higher resolution, sample throughput declines in inverse ratio to the resolution. The relationship is typical, i.e., the product of processing rate and resolution for a given buffer conductivity tends to be a constant. This product (equal to 300 in Fig. 1), is a useful "figure of merit" for performance, since either high throughput alone (with very low resolution) or high resolution alone (at near-zero throughput) will be of limited value. The performance level shown for 1 *g* is useful and, for many purposes, adequate. In terms of processing rate, it is limited however, being, relatively speaking, a micro method. It has been proposed that the processing rate be increased by operation in microgravity using a greater cell thickness. This appears quite feasible. We will show, however, that the proposed DLE approach could enhance performance by a much larger factor, making available a new area of capability represented by the shaded zone of Fig. 1. Useful levels of resolution could be combined with processing rates perhaps 25- to 100-fold greater than now possible at 1 *g* for comparable resolution.

The validity of the proposed approach is contingent on showing that moderately thick liquid layers, subject to specified levels of electrical heating, will maintain laminar flow stability in zero gravity. The proposed investigation must verify such stability in one or more space flights, using layers of different thickness and appropriate combinations of flow velocity and heating level. This would supplement theoretical predictions and introduce into a real device the design variables that may be intractable to theory.

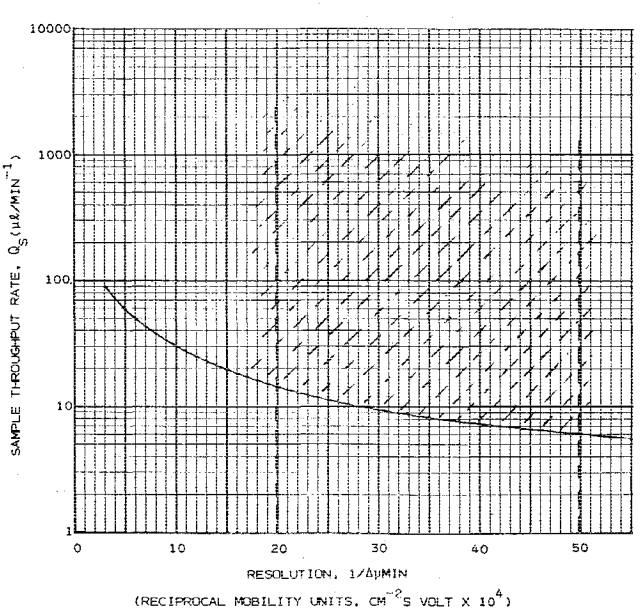

Fig. 1 Performance relationships in continuous flow electrophoresis.

Presented as Paper 77-233 at the AIAA 15th Aerospace Sciences Meeting, Los Angeles, Calif., Jan. 24-26, 1977; submitted Feb. 1, 1977; revision received Feb. 3, 1978.

Index category: Space Processing.

*Senior Scientist, Advanced Technology Operations.

Technical Discussion

Principle of DLE

The arrangement in conventional continuous electrophoresis (CCE) of the planar type is shown in Fig. 2a. A layer of buffer flows downward under laminar flow conditions between parallel plates. Before the electric field is applied, the fine sample stream introduced at A descends in a straight line to B. When a lateral field is applied by a pair of electrodes as shown, sample components of different mobility are deflected at different angles, forming a steady-state fan. Separate components are withdrawn from positions such as C, D, E, and F. In deflected-laminar electrophoresis (DLE) (Fig. 2b), the sample mixture is introduced as a thin sheet, starting, for example, at AB and, in the absence of a field, terminating at CD. On applying a field face-to-face across the layer, each separated component forms its own steady-state thin layer of material such as ABFE. An advantage inherent in DLE is the capacity for processing the sample at a much higher rate than the conventional system, since the sample is introduced as a broad band rather than a thin filament.

The concept of applying a field normal to a plane of sample flowing in a uniform buffer layer has appeared from time to time in various forms. Examples are the work of Dobry and Finn[5] and Bier.[6] However, the reported results showed limited performance and left unexplained various factors affecting the capability of such systems. Among these were the effect of the velocity profile in the buffer layer, electroosmotic effects, and change in buffer properties (e.g., pH and conductivity) adjacent to the membranes. The limitations in reported performance, combined with insufficient understanding of the underlying phenomena, have apparently discouraged serious consideration of a DLE approach to space processing.

Recent studies and new techniques justify a reassessment of the DLE approach. Provided that laminar flow stability in microgravity can be demonstrated in buffer layers 4 mm or more thick, subject to useful electric field strengths, DLE offers the promise of remarkable new levels of performance.

Analysis of DLE

Unit Cell

In comparing DLE with the conventional continuous method, a convenient starting point is the concept of a "unit cell" (Fig. 3a). The square cross section ABCD is that of a hypothetical cell with buffer flowing downward, i.e., normal to the drawing plane. Electrodes (dotted lines) at BA and CD apply a dc field, and J is the sample stream cross section prior to electrophoresis. If in Fig. 3b we stretch the cross section to give contour ABGH with electrodes at BA and GH, we define a CCE system. If we stretch the cross section, and the electrodes as well, at right angles to this direction, giving contour AEFD, we define the DLE system. Given an aspect ratio (ratio of thickness to breadth) equal to unity in the unit cell, the distinction between DLE and CCE disappears. How, then, is performance affected by extension in the two different directions? We assume the height of the cell (perpendicular to the drawing) equal for both cases, i.e., the practical maximum from a physical or engineering point of view. We assume also the same buffer, of given conductivity, and the same maximum tolerable internal buffer temperature.

CCE Performance

We are concerned with two aspects of the performance: sample volume processing rate Q_s' and resolution R. For CCE, the first is approximated by

$$Q_s' = D\Delta X_s V_0 \tag{1}$$

where D is the cell thickness, ΔX_s the initial thickness of the sample stream, and V_0 the buffer layer velocity. Resolution may be defined as the reciprocal of the least mobility difference $\Delta\mu_e$ resolvable by the system, or

$$R = 1/\Delta\mu_e = X_t/(\mu_t \Delta X_s) \tag{2}$$

where X_t is the displacement, after traversing the field zone, of the most mobile component, and μ_t the mobility of that component.

Taking as the figure of merit for performance the product $Q_s'R$, we have from Eqs. (1) and (2)

$$Q_s'R = DV_0X_t/\mu_t \tag{3}$$

However,

$$X_t = \mu_t EH/V_0 \tag{4}$$

where E is the electric field gradient and H the field zone dimension (height) in the buffer flow direction. This gives for the figure of merit

$$Q_s'R = DEH \tag{5}$$

For any given buffer conductivity, the temperature elevation in the curtain is proportional to D^2E^2. Therefore, once we reach the maximum buffer temperature tolerated by the sample, or an onset of convective disturbance caused by the temperature rise (H being already the practical maximum), the figure of merit, Eq. (5), can no longer be increased. In this sense, CCE is a performance-limited system.

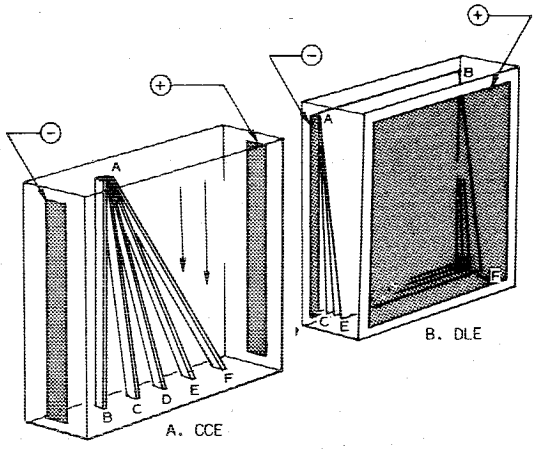

Fig. 2 Configurations of conventional continuous electrophoresis (CCE) and deflected-lamina electrophoresis (DLE).

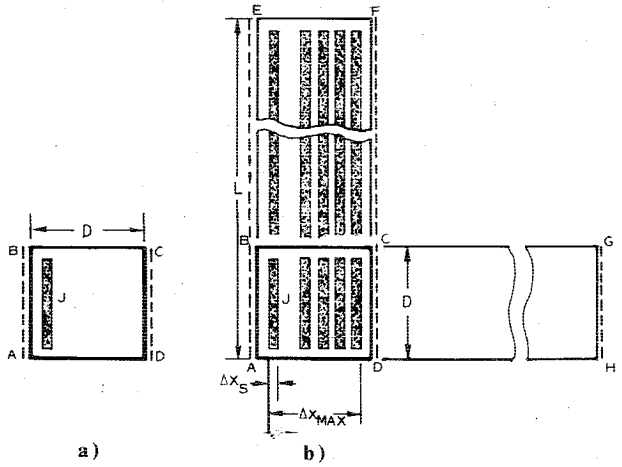

Fig. 3 a) Unit cell and b) comparison of DLE and CCE.

It has been proposed that the performance limit be increased by operating the conventional system in space. Thus, the cell thickness D (and the product DE) could be increased (compared with the performance on Earth) before convection set in. This is true; however, the sample throughput would be increased only in direct proportion to D, assuming resolution is kept constant. Accordingly, only a moderate increase in processing rate, say four to seven fold, could be anticipated.

Considering resolution per se, however, we note in CCE that elongation of the cell cross section beyond the dimension D (to GH in the figure) can be useful. Thus, considering the maximum deflection, defined by Eq. (4) and resolution R defined by Eq. (2), the additional space may accommodate higher X_t values, with increase of resolution, by reducing the buffer velocity V_0. Sample throughput rate is, of course, decreased in the same ratio. Alternatively, one could reduce the cell thickness D, allowing higher E values and increased deflection while maintaining temperature elevation unchanged. Again, the processing rate is reduced in proportion to D. These conditions show that resolution per se in CCE can, in principle, be increased indefinitely.

DLE Performance

Considering now the DLE system, we find that sample processing rate is approximated by

$$Q_s' = L\Delta X_s V_0 \tag{6}$$

where L is the cell breadth as shown in Fig. 3b. Resolution, as for CCE, is given by Eq. (2). Combining Eqs. (6) and (2) for the figure of merit,

$$Q_s' R = X_t L V_0 / \mu_t \tag{7}$$

But X_t, the maximum possible deflection, may be equated with the available cell thickness D, and expressed as

$$D = \mu_t E H / V_0 \tag{8}$$

giving for the figure of merit

$$Q_s' R = LEH \tag{9}$$

Comparing this with the corresponding expression for CCE, we note in Eq. (9) that, although for given buffer conductivity the field gradient E has an upper limit set by tolerable temperature or convection disturbance, L has no such limitation. Increasing L is without effect on temperature elevation in the cell, since it increases neither the heat generation rate per unit of buffer volume nor heating rate per unit of cell area.

Comparing Eqs. (5) and (9), we see that the DLE figure of merit exceeds that of CCE by the ratio L/D. Actually, the sample stream in the CCE cannot occupy the full cell thickness D. If it did, bands of sample components other than that matching the cell wall in zeta potential would be greatly broadened, due to flow profile and electroosmotic effects, and resolution for most of the pattern seriously degraded.[3] The useful fraction of cell thickness occupied by the sample in CCE ranges from perhaps one-fifth to one-half. Thus, the actual performance advantage of DLE over CCE is about $2L/D$ to $5L/D$. Assuming that microgravity allows D to be as large as 0.5 cm, each centimeter of cell width L in a DLE would increase the figure of merit five to ten-fold.

Excessive extension of the dimension L in DLE introduces new problems, however, since nonuniformity of the field or the cell thickness may then begin to degrade resolution.

Resolution in DLE System

A principal question in DLE is whether the available thickness D, as enlarged in microgravity, will suffice to accommodate the number of "slices" n to be resolved in the mobility spectra of real samples. This number is approximated by the relations

$$n = D/\Delta X_s = \mu_t/\Delta\mu_e \tag{10}$$

We imply here that the width of an electrophoretically homogeneous component band on leaving the field zone equals the initial sample bandwidth. This is justified for typical biological particles such as cells, where broadening due to Brownian or thermal diffusion is negligible. In the Einstein diffusion equation, the root-mean-square $\overline{\Delta X}$ of broadening during time t is

$$\overline{\Delta X} = (2\delta t)^{1/2} \tag{11}$$

where δ is the diffusion constant. For an assumed 5-μm-diam particle, δ is about 1×10^{-9} cm^{2}s^{-1}, and $\overline{\Delta X}$ is 6 μm for an assumed $t = 180$ s. For smaller diameter particles, δ will vary inversely as the diameter and $\overline{\Delta X}$ will vary as the inverse square root of the diameter. Now, in Eq. (10), recalling that μ_t is the mobility of the most mobile component and $\Delta\mu_e$ the minimum mobility difference to be resolved, we see that DLE is not limited in resolution as such, since both μ_t and $\Delta\mu_e$ may be very small values. The ratio $\mu_t/\Delta\mu_e$ may not be too large, however, since DLE is an "n-limited" system.

We examine first what values of n appear achievable in DLE, then compare these with values required for real biological separations. First it appears easily possible to make the sample band as thin as 0.02 cm, a value proposed for preliminary flight tests. It appears feasible later to make this as thin as 0.01 cm. For dimension D, we have proposed, as a conservative enlargement over the maximum 1 g value of 0.15 cm, a value of 0.45 cm for initial flight tests. Later experience in microgravity may show that this can be increased to 0.6 cm or more. Within these reasonable limits for ΔX_s and D, we have an n-range, as shown in Table 1, from 22.5 to 60.

Considering the requirements of actual separations, Seaman[4] has cited, as a desirable ultimate value, a resolvable mobility difference of 0.02 mobility unit (μm/s per V/cm). His stated acceptable value is 0.05 unit. (These limits are designated by vertical dotted lines in Fig. 1.) This translates into required n values per Eq. (10) by taking representative maximum mobility values μ_t in real samples. Again, from the work of Seaman, a mixed erythrocyte sample (human, canine, chicken) was considered representative of a relatively low mobility sample. The maximum mobility μ_t in standard saline is -1.25 units, and in a typical 0.01 M buffer (pH 7.25), about -2.1 units. Taking into account the natural scatter of mobility in each band, imagine a requirement for splitting one of the bands into ten mobility increments (for example, to separate old from young cells). For the average erythrocyte band this requires a resolvable mobility difference $\Delta\mu_s$ of 0.04 units, and from the relation $n = \mu_t/\Delta\mu_e$, we have $n = 31$. For the same cells in the 0.01 M buffer, μ_t and $\Delta\mu_e$ are proportionately increased, and if ten slices per band again suffice, n is unchanged.

As a second sample, again from an analytical electrophoresis experiment by Seaman,[7] we note for a kidney cell population a maximum mobility μ_t in the 0.01 M buffer of -2.3 units. The mobility increments are 0.05 mobility unit, and n in his work is $2.3/0.05 = 46$. These examples are summarized in Table 2.

Table 1 n as a function of ΔX_s and D

ΔX_s, cm	D, cm	$n (= D/\Delta X_s)$
0.02	0.45	22.5
0.02	0.60	30
0.015	0.45	30
0.015	0.60	40
0.010	0.45	45
0.010	0.60	60

Table 2 Examples of required n values

	μ_t [a]	$\Delta\mu_e$ [a]	$n=\frac{\mu_t}{\Delta\mu_e}$
Erythrocytes, mixed, in standard saline	1.25	0.4	31
Erythrocytes, mixed, in 0.01 M buffer (pH 7.25)	2.13	0.07	30
Mixed kidney cells	2.3	0.05	46

[a] Mobility units.

Study of published data on mobility distributions of many other kinds of biological particle mixtures indicates a comparable range of required n values.

The required n ranges are fully compatible with feasible ranges for DLE in microgravity. Granting there may be occasional unusual resolution requirements, for example a combined maximum mobility (μ_t) value of 3.5 mobility units and a required resolvable difference of 0.035 unit (or $n=100$), this performance level may still be achievable. For example, it may be feasible in microgravity to have a cell thickness D of 1.0 cm combined with a sample band thickness of 0.01 mm.

Energy Efficiency

The DLE system is far more efficient than the CCE in electrical energy expended per unit of sample processed. Within the electrophoresis space itself, given the same buffer width, thickness, and voltage gradient, the improvement factor is the same as for the figure of merit, i.e., about $2L/D$ to $5L/D$. However, since in the DLE a somewhat higher proportion of total wattage is expended in the electrode chambers, overall improvement is about 0.8 times the above or about $1.6L/D$ to $4L/D$.

Trajectory Equation

In CCE, a given sample particle remains at a constant depth in the buffer while traversing the cell. Its longitudinal velocity dy/dt (equal to that of the liquid at the depth of the particle) and transverse (electrophoretic) velocity dx/dt are both constant. The particle trajectory is therefore a straight line deflected from the curtain flow direction by an angle α where

$$\tan\alpha=\frac{dx}{dt}\Big/\frac{dy}{dt} \tag{12}$$

In DLE, however, with the field applied normal to the flow plane, each particle experiences a changing longitudinal velocity, described by the velocity profile of the medium, as it is progressively deflected. It was of interest to know how seriously this would distort the sample trajectories and affect system performance.

If in a side view of the cell (Fig. 4), we define cell middepth as $x=0$ with wall positions at $x=\pm d$ and the middepth velocity as V_0 then neglecting temperature dependence of viscosity, the longitudinal velocity varies with depth as

$$\frac{dy}{dt}=V_0\left(1-\frac{x^2}{d^2}\right) \tag{13}$$

The transverse particle velocity, proportional to the electrophoretic mobility of the particle and the electric field gradient, is simply the electrophoretic velocity u_e:

$$\frac{dx}{dt}=u_e(\text{const}) \tag{14}$$

From the ratio of Eqs. (13) and (14)

$$\frac{dy}{dx}=V_0\frac{[1-(x^2/d^2)]}{u_e} \tag{15}$$

Integrating and taking constants such that $y=0$ at $x=x_i$, we obtain for the trajectory the cubic equation

$$y=\frac{V_0}{u_e}\left(\frac{x_i^3-x^3}{3d^2}+x-x_i\right) \tag{16}$$

Figures 5a-c are computer plots of this equation for three lateral positions, x_i, of sample injection. In each figure, the multiple trajectories represent seven components of different electrophoretic velocity u_e such that the outer bands just intercept the cell wall and the others are equally spaced at the lower edge of the field. The aspect ratio shown for the cell cross section is arbitrary and without effect on the relative form of the trajectories or the relative band displacements.

It was gratifying to observe that, except where injection or collection positions approach the cell walls, the trajectories are nearly straight lines. In practice, operating conditions and

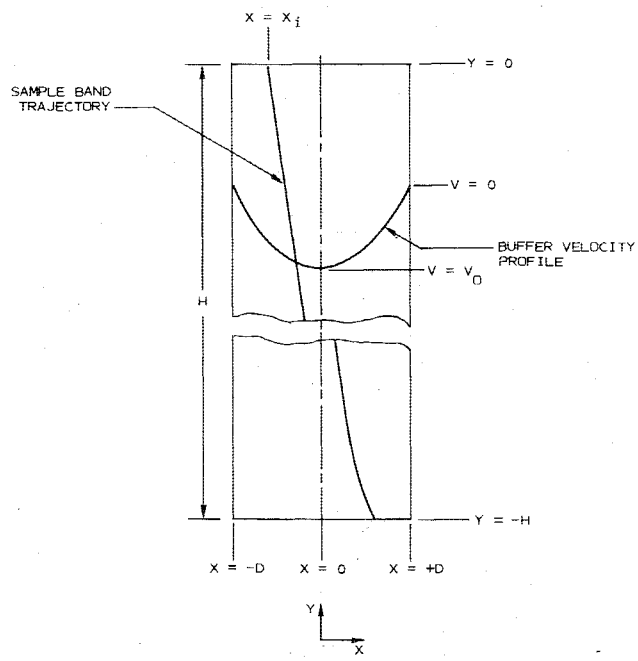

Fig. 4 DLE cell profile relationships.

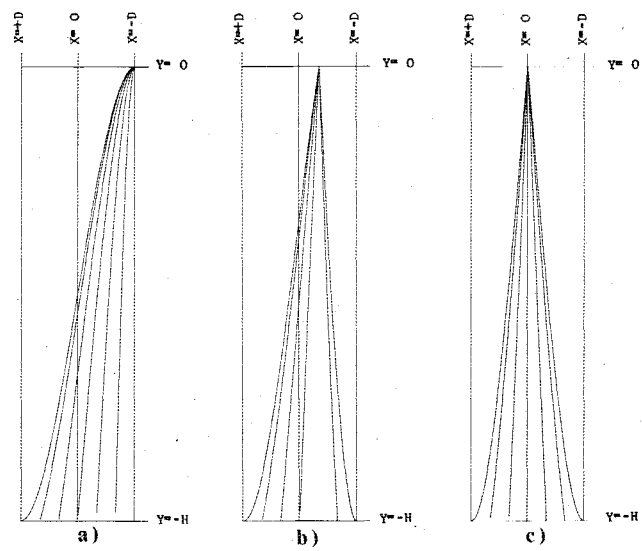

Fig. 5 DLE component band trajectories.

length of the field zone would be such that the outer bands do not reach the walls before leaving the field. Further, since the electric field at the lower end of the field zone tends to fade gently rather than terminate sharply, the ends of the trajectories round off into the flow direction rather than change direction abruptly.

Deflection as a Function of Relative Mobility

Unlike the case in CCE, the lateral deflection is not a linear function of the mobility or electrophoretic velocity. To define this function, we derive the general expression for x at $y=-H$, where H is the effective field length. Denoting this final intercept value of x as x_f, then equating y in Eq. (16) to $-H$ and rearranging, we have

$$x_f^3-3d^2x_f-(x_i^3-3d^2x_i+3d^2u_eH/V_0)=0 \tag{17}$$

Before solving for x_f, we redefine the electrophoretic velocity as a relative value, i.e., as a proportional value within the range of electrophoretic velocities accommodated by the cell. Being dimensionless, this value may also be interpreted as relative mobility. The limiting electrophoretic velocities $u_{\min}$ and $u_{\max}$ are those giving trajectories just touching the wall at the end of the field zone.

The bands of limiting electrophoretic velocity pass through the points $(-H, -d)$ and $(-H, +d)$, respectively. Substituting these coordinates in Eq. (16) and solving for the limiting velocities, we find

$$u_{e_{\max}}=-\frac{V_0}{3d^2H}(x_i^3-3d^2x_i+2d^3) \tag{18}$$

$$u_{e_{\min}}=-\frac{V_0}{3d^2H}(x_i^3-3d^2x_i-2d^3) \tag{19}$$

The accommodated electrophoretic velocity range is

$$u_{e_{\max}}-u_{e_{\min}}=-\frac{4}{3}\frac{V_0d}{H} \tag{20}$$

Defining now the relative electrophoretic velocity (or mobility) u_{er} of any component as

$$u_{er}=(u_e-u_{e_{\min}})/(u_{e_{\max}}-u_{e_{\min}}) \tag{21}$$

we have

$$u_e=\frac{u_{er}}{u_{e_{\max}}-u_{e_{\min}}}+u_{e_{\min}} \tag{22}$$

and by combining Eqs. (22) and (20) with Eq. (17),

$$x_f^3-3d^2x_f+4d^3u_{er}-2d^3=0 \tag{23}$$

Solving Eq. (23) for x_f, we obtain as the appropriate root, in trigonometric form

$$x_f=2d\cos\left(\frac{\arccos(1-2u_{er})}{3}+240\ \text{deg}\right) \tag{24}$$

The plot of x_f as a function of u_{er} is presented in Fig. 6. The properties of this function are most interesting. First, in practical terms, the function is essentially a straight line for about 70% of the relative mobility range. The slope in this region is the same as in CCE for equivalent relative mobilities. The curve is independent of the lateral position x_i of sample injection. Outside the "linear" range, for components of lowest and highest mobilities, the rate of deflection increases and resolution is somewhat improved. As a result of the increased deflection for the outer bands, the total range of mobility accommodated, Eq. (20), is less than in a CCE system of equivalent dimensions by a ratio 2/3 to 1.

Elimination of Electro-osmosis

One of the advantages of the DLE approach is the expected disappearance of electro-osmotic effects. In any free electrophoresis system, these effects arise along cell wall surfaces oriented parallel to the field direction (i.e., the direction of current flow) and comprise a movement of counter-ions and associated solute through the field gradient. Since in DLE the cell walls and their counter-ion layers lie essentially in equipotential planes, electro-osmosis is not expected to occur. To prevent electro-osmosis at the surfaces forming the *edges* of the cell, the buffer layer is merely extended some distance beyond the edges of the field zone. With electro-osmosis eliminated, resolution should be essentially uniform for all component bands, unlike the situation in CCE where curvature of the band cross section reduces resolution for all but the "focused" portion of the pattern.[3]

Electrolytic Gas Generation

Electrolytic gas generation rates in DLE are relatively high, but only in the proportion that DLE has the higher figure of merit. Consider a volume of buffer H cm high, L cm wide, and D cm thick, with an electrical conductivity K_e. We subject this volume to a voltage gradient E in two alternative ways: 1) by applying the field edge-to-edge, i.e., across dimension L (conventional method); and 2) applying the field face-to-face, across dimension D (DLE approach).

If we neglect secondary effects, such as temperature-dependence of electrical and thermal conductivity, and assume the same boundary temperatures, then the internal temperatures and temperature gradients will be the same, if the field gradient E is the same. However, the applied voltage necessary to generate this gradient, and the resulting current through the buffer, may be very different. The conductances K_1 and K_2 of the buffer volume in the respective cases are:

$$K_1=K_eDH/L \tag{25}$$

$$K_2=K_eLH/D \tag{26}$$

The respective currents are

$$I_1=V_1K_1 \tag{27}$$

$$I_2=V_2K_2 \tag{28}$$

where V_1 and V_2 are the respective voltages to be applied, namely,

$$V_1=EL \tag{29}$$

$$V_2=ED \tag{30}$$

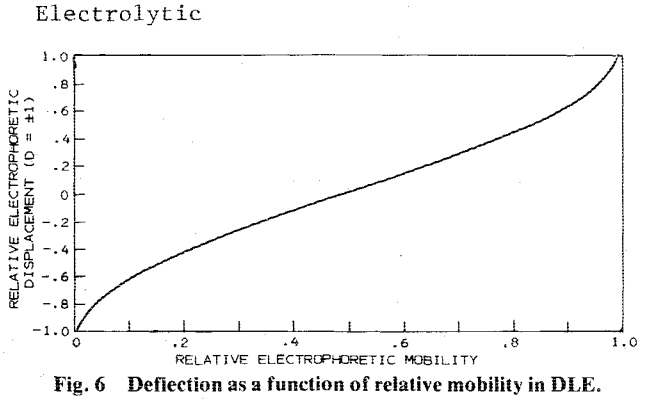

Fig. 6 Deflection as a function of relative mobility in DLE.

Combining Eq. (27) with Eqs. (25) and (29), then Eq. (28) with Eqs. (26) and (30), and taking the ratio of currents, we find

$$I_2/I_1 = L/D \tag{31}$$

By Faraday's law, the gas generation rates are generally proportional to the current. Further, we showed earlier that L/D is precisely the advantage ratio in figure of merit of DLE over CCE. Accordingly, gas generation in DLE is increased over conventional values only in the ratio that DLE enhances performance.

Reynolds Limit Considerations

The flow velocities contemplated in DLE imply Reynolds numbers far below the turbulence limit. The dimensionless Reynolds number R is defined as

$$R = \rho V N/\eta \tag{32}$$

where ρ is the density, V the average velocity in the channel, η the viscosity, and N a "characteristic dimension" defined as

$$N = 4A/C \tag{33}$$

where A is the area of the cross section and C the circumference. For a rectangular channel having a breadth large compared with its thickness D,

$$N \simeq 2D \tag{34}$$

Substituting Eq. (34) in Eq. (32),

$$R = 2\rho VD/\eta \tag{35}$$

The turbulence limit for R is about 2000. In our own systems, with viscosity equal to approximately 0.01 P, ρ about 1.0 g/cm^3, and D and V having values of 1 cm and 1 cm/s, approximately as maxima, R has a maximum value of about 200.

Design Problems and Approaches

The DLE approach poses several distinctive design problems. These stem from the narrow deflection space, the width of the sample band, and the need for extended electrode areas which must also serve as cooling surfaces.

Area Electrodes

In the proposed design, the electrode assemblies form removable inserts in the front and rear cell plates (Fig. 7). Their structure is further detailed in Fig. 8. The electrode comprises a grid of platinum wires threaded through parallel grooves in the insert surface. The grooves serve as channels for crossflow of cold, circulating electrode rinse medium, usually of the same composition as the electrophoresis buffer. The rinse fluid removes both electrolytically generated ionic and gaseous products and heat generated in the electrophoresis space. The small pore microporous membranes covering the grooves prevent disturbance of the electrophoresis medium by the rinse fluid, while providing ionic communication between these two media. Conductivity and pH changes near the membrane surface are also minimal with this material.

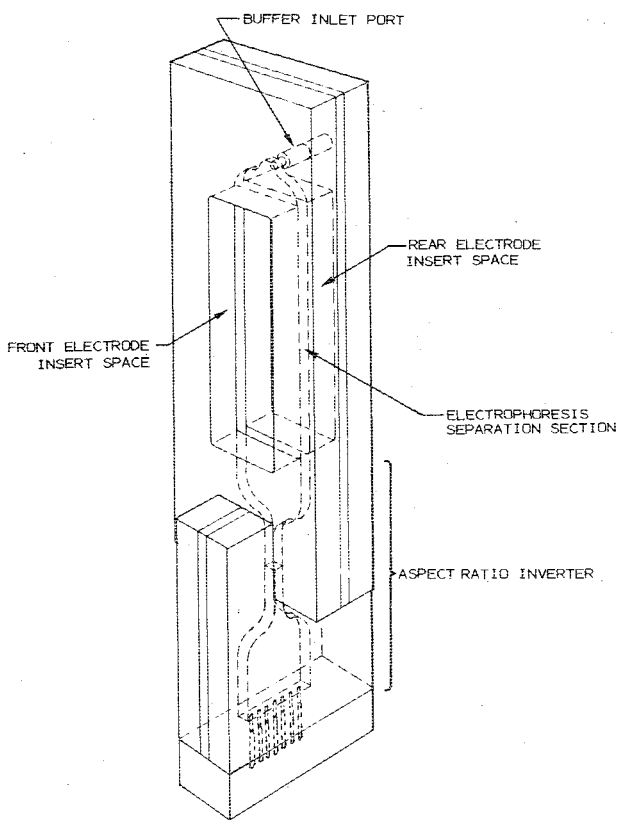

Fig. 7 Proposed flight prototype cell.

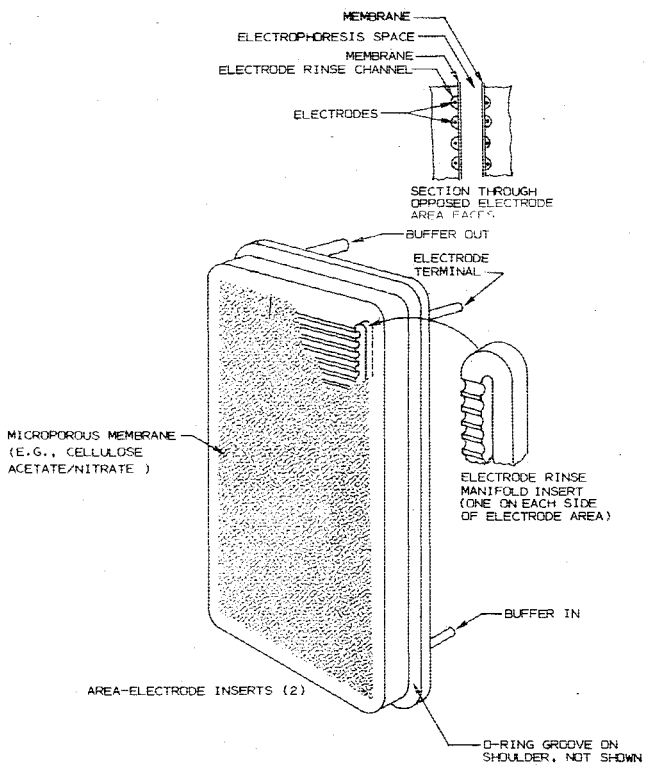

Fig. 8 Insertable area-electrode panel.

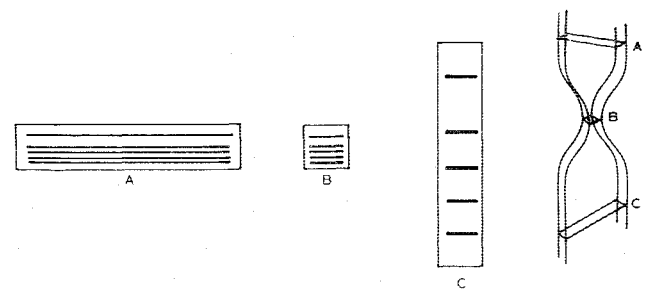

Fig. 9 Transformation of separation patterns in the aspect ratio inverter (ARI). Illustrated are the separated bands at levels A, B, and C of the DLE apparatus.

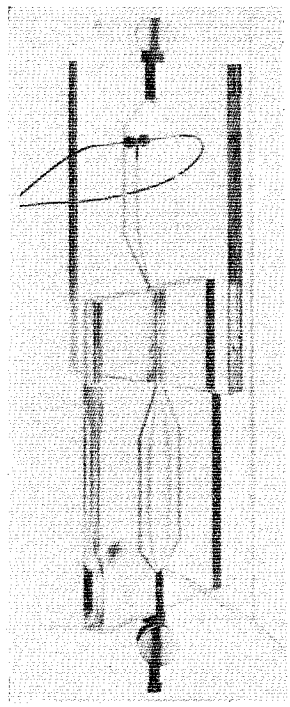

Fig. 10 Demonstration of aspect ratio inversion.

Fraction Collection: ARI Technique

The delivery of fractions from the DLE chamber in the unusual form of broad, closely spaced bands poses a problem in fraction collection, since the process must not degrade the resolution achieved in the chamber. We have proposed as a solution to this problem a novel aspect ratio inversion technique, as illustrated in Fig. 9.

As the buffer layer leaves the field zone, with its broad separated leaves of sample components, its width is narrowed to form an approximately square cross section. This cross section is then again broadened, but at right angles to the buffer plane in the cell above. In effect, the aspect ratio has been inverted—the width of the buffer layer has become the thickness and vice versa.

The transformation of the band cross section is illustrated by Fig. 9. This shows (Fig. 9a) their appearance just after leaving the field zone, the appearance (Fig. 9b) in the narrowed, square lumen, and, finally (Fig. 9c), the configuration after rebroadening. In this last form, the bands may be conveniently collected in the usual way via a linear array of collector tubes.

The ARI concept has been successfully tested in a laboratory model. The results are shown in Fig. 10. Constructed of Plexiglas (a product of Rohm and Haas), it comprises two "sandwich" panels, each formed by three cemented layers. The middle layer of each provides a parallel-sided flow zone (1 in. wide, ⅛ in. thick), tapering into a square (⅛ × ⅛ in.) intermediate cross section. Rectangular notches, cut part way into the end of each assembly and

Table 3 Cell design and operating parameters

Symbol	Variable	Units	High watt/ high flow	Low watt/ low flow	High K_e
Z	Width of field zone (z dimension)	cm	2.0	2.0	2.0
L	width of buffer layer (z dimension)	cm	3.0	3.0	3.0
Z_s	Width of injected sample layer (z dimension)	cm	1.5	1.5	1.5
X_s	Thickness of injected sample layer	cm	0.01	0.01	0.01
$2d$	Thickness of buffer layer	cm	0.2	0.2	0.6
H	Length of field zone (y dimension)	cm	10.0	10.0	40.0
Q_s'	Sample volume injection rate	mliter/min	0.59	0.24	0.36
Q_c'	Buffer volume flow rate	mliter/min	15.8	6.3	28.8
V_0	Buffer midplane velocity	cm/s	0.66	0.26	0.40
t	Sample transit time through field zone	s	15.2	38.1	100.0
K_e	Electrical conductivity of buffer	ohm^{-1} cm^{-1}	650×10^{-6}	600×10^{-6}	1.5×10^{-2}
E	Voltage gradient across buffer layer	V/cm	93.9	43.7	13.2
V_t	Voltage applied to cell	V	46.5	21.9	10.9
I	Cell current	A	1.22	0.53	15.84
W_c	Watts dissipated in field zone	W	22.9	4.59	125
W_t	Watts, total, including dissipation at electrodes	W	56.8	11.5	188
E^2K_e	Watts per unit of cell buffer volume	W/cm^3	5.73	1.15	2.6
T_{max}	Maximum (midlayer) buffer temperature	°C	10	6	20
T_w	Temperature at buffer/cell wall interface	°C	5	5	5
X_t	Electrophoretic displacement of most mobile component	cm	0.1	0.1	0.3
μ_t	Mobility of most mobile component	μm s^{-1} cm V^{-1}	0.7	0.7	0.6
$\Delta\mu_e$	Least resolved mobility difference	μm s^{-1} cm V^{-1}	0.07	0.06	0.02
n	Number of resolvable bands	–	10	10	30
Q_c'	Volume rates of H_2, O_2 gas generation	mliter/min	H_2: 9.34 O_2: 4.67	H_2: 4.06 O_2: 2.03	121.21 60.6

leaving the square aperture, allow mating and hermetic sealing at mutual right angles as shown.

To insure laminar flow in our 1-*g* apparatus, a slightly viscous flow medium (water plus glycerine) was used. The apparatus was not designed to perform an electrophoresis but to test the ARI concept per se. Accordingly, preseparated bands were injected at a steady flow rate. To simplify the experiment, these entered as point-samples rather than as broad bands, representing adjacent points lying in hypothetical, closely adjacent layers. By the ARI process, the two "sub-bands," lying at different depths but at the same lateral position in the upper section, are transformed to appear at the same depth but different lateral positions in the lower section.

The injected streams were India ink diluted with flow medium. The diameter of the injected streams was 0.012 in., the linear velocity in the broad cell sections 2 in./min.

Design of a Flight Experiment

System Configuration

A rocket flight experiment embodying concepts and design approaches previously described has been proposed to NASA. Its objectives are, first, to verify that a buffer layer of useful thickness will maintain stable laminar flow in microgravity at prescribed levels of electrical heating and flow velocity. Second, the experiment will test the validity of the DLE cell concept and design in microgravity by separating a biological mixture, for example fixed red blood cells.

Prior experiments will have assessed, to the extent possible at 1 *g*, the stability of the flowing buffer layer, electro-osmotic effects, buffer alteration at the membrances, and integrity of the electrode structure.

The rocket flight system provides for continuous sample and buffer feed from motor-driven syringes, collection of fractions in expandable sacs immersed in a water-filled compartment, chilling of the electrode rinse medium in a heat exchanger, separation of electrolytic gases from the rinse medium, and photographic monitoring of the transilluminated separation pattern. The entire assembly is enclosed in a nitrogen- or helium-filled cylindrical shell.

An electronic subassembly provides power supplies, housekeeping electronics, and programmed control of the operational sequence.

Cell Dimensions and Operating Parameters

The proposed system operates under two sets of conditions during a single flight: high watt/high flow (HW-HF) and low watt/low flow (LW-LF). Dimensional and operating values are shown in Table 3 (exclusive of the last column). The general geometry of the cell is shown in Fig. 7.

The HW-HF and LW-LF experiments represent different separation requirements. In the HW-HF, the sample could be of a type relatively tolerant to elevated temperature; in the LW-LF experiment it might be less so. Sample components illustrated in both cases are of relatively low mobility and have comparable resolution requirement. In effect, with the slower curtain in the LW-LF case, we trade sample throughput rate for lower temperature operation.

For calculation of values in Table 3, simplifying assumptions were made that slightly alter the true values. Electrical conductivity in the buffer was assumed constant, independent of temperature variation in the buffer cross section. Thermal conductivity and viscosity of the buffer were likewise assumed temperature independent. Steady-state thermal conditions were assumed throughout the field zone, i.e., for a fluid element anywhere in the field, heat loss by conduction was assumed constantly equal to heat gain.

The design and operating values shown, appropriate to an early rocket flight, are conservative. The short field zone length (10 cm) could in a later system be multiplied severalfold. It may prove possible later to increase the buffer layer thickness from 0.2 cm to perhaps 0.6 cm or more. Conservative maximum temperatures are shown, whereas many samples could tolerate temperatures up to 35°C during the short transit times involved. Accordingly, a severalfold improvement in resolution and/or throughput may be expected. Nevertheless, the values shown for the rocket test already represent useful resolution combined with sample processing rates about ten-fold greater than seen in conventional 1-*g* techniques.

In extrapolating the data of Table 3 to possible levels of future performance, the following relationships are applicable:

1) Increasing the field length H increases sample processing rate or absolute resolution $\Delta\mu_e$ in the same proportion; it does not per se increase n.

2) Increasing the buffer layer thickness increases n, the number of resolvable fractions, in the same proportion.

3) Increasing the allowed temperature elevation ($T_{max} - T_w$) can increase the sample processing rate or absolute resolution as the square root of the temperature elevation increase by allowing application of a higher voltage gradient E.

4) Increasing the width of the buffer layer (D, equal to $2d$) will increase the sample processing rate in the same proportion.

It is apparent, then, that simple extension of length and width, both reasonably possible in future facilities such as shuttle, can further increase the performance figures (in resolution and/or throughput) by about five- to ten-fold. Depending also on results of future space experiments which may validate the use of thicker and warmer buffer layers, still another increase in performance of about two-fold may be attainable.

The high figure of merit of DLE may also permit a tradeoff providing a different and valuable new capability, i.e., electrophoresis in buffers of high conductivity approximating that of physiological media. This would offer a new freedom in the design of buffer compositions. At present, the design of low-conductivity buffers necessary for low-heating effect is often tedious, may compromise cell viability, and cause adsorption or aggregation effects that seriously degrade the resolution. The tradeoff results in a lower but nevertheless useful sample processing rate. A hypothetical future example is illustrated by the values in the last column of Table 3. A relatively thick buffer layer is indicated, as is a relatively high-temperature elevation. The processing rate is lower by about five-fold than would be possible with lower conductivity buffer (e.g., $K_e = 600 \times 10^{-6}$ ohm^{-1} cm^{-1}), assuming equal allowed temperature elevation and equal buffer layer thickness.

References

[1] Barrolier, V. J., Watzke, E., and Gibian, H., *Zeitschrift fuer Naturforschung*, Vol. 13(b), 1958, p. 754.

[2] Hannig, K., *Zeitschrift fuer Analytische Chemie*, Vol. 181, 1961, p. 244.

[3] Strickler, A. and Sacks, T., *Annals of New York Academy of Sciences*, Vol. 209, 1973, p. 497.

[4] Seaman, G. V. F, personal communication, 1975.

[5] Dobry, R. and Finn, R. K., *Science*, Vol. 127, 1958, p. 697.

[6] Bier, M., Smolka, A. J. K., Kapwillen, A., and Ostrach, S., *Journal of Colloid and Interface Science*, Vol. 55, 1976, p. 197.

[7] Seaman, G. V. F., personal communication, 1976.